

DYRK1A and Glycogen Synthase Kinase 3 β , a Dual-Kinase Mechanism Directing Proteasomal Degradation of CRY2 for Circadian Timekeeping[∇]§

Nobuhiro Kurabayashi, Tsuyoshi Hirota,[†] Mihoko Sakai, Kamon Sanada,[‡] and Yoshitaka Fukada*

Department of Biophysics and Biochemistry, Graduate School of Science, University of Tokyo, Hongo 7-3-1, Bunkyo-ku, Tokyo 113-0033, Japan

Received 7 August 2009/Returned for modification 20 October 2009/Accepted 18 January 2010

Circadian molecular oscillation is generated by a transcription/translation-based feedback loop in which CRY proteins play critical roles as potent inhibitors for E-box-dependent clock gene expression. Although CRY2 undergoes rhythmic phosphorylation in its C-terminal tail, structurally distinct from the CRY1 tail, little is understood about how protein kinase(s) controls the CRY2-specific phosphorylation and contributes to the molecular clockwork. Here we found that Ser557 in the C-terminal tail of CRY2 is phosphorylated by DYRK1A as a priming kinase for subsequent GSK-3 β (glycogen synthase kinase 3 β)-mediated phosphorylation of Ser553, which leads to proteasomal degradation of CRY2. In the mouse liver, DYRK1A kinase activity toward Ser557 of CRY2 showed circadian variation, with its peak in the accumulating phase of CRY2 protein. Knockdown of *Dyrk1a* caused abnormal accumulation of cytosolic CRY2, advancing the timing of a nuclear increase of CRY2, and shortened the period length of the cellular circadian rhythm. Expression of an S557A/S553A mutant of CRY2 phenocopied the effect of *Dyrk1a* knockdown in terms of the circadian period length of the cellular clock. DYRK1A is a novel clock component cooperating with GSK-3 β and governs the Ser557 phosphorylation-triggered degradation of CRY2.

Circadian rhythms with a period of approximately 24 h are generated by biological clocks, which continue to oscillate even in the absence of external time cues (5, 33). In mammals, central clock genes, such as *Clock*, *Bmal1*, and a set of *Per* (*Period*) and *Cry* (*Cryptochrome*) genes, form a transcription/translation-based feedback loop to generate a stable circadian oscillation of the molecular clock (15, 27). A heterodimer of CLOCK and BMAL1 activates transcription of the *Per* and *Cry* genes through binding to E-box enhancer elements in their promoters (3, 11). Translated PER and CRY proteins then associate with each other to translocate to the nucleus, where they inhibit their own transcription by interacting with CLOCK-BMAL1 dimer (22, 30). This negative limb of the transcriptional regulation, causing reduction of *Per* and *Cry* mRNA levels, is accompanied by fine-tuned degradation of the PER and CRY proteins, allowing the molecular cycle to start again with activation of the E-box-dependent transcription the next day.

In addition to transcriptional and translational regulation, circadian properties of the clock oscillation depend heavily on

posttranslational modifications, especially phosphorylation of clock proteins (reviewed in reference 10). For example, it has been reported that CKI δ (casein kinase 1 δ) and CKI ϵ bind to and phosphorylate PER proteins, thereby regulating their degradation and subcellular localization (1, 6, 31, 34, 38). In humans, two types of dominant FASPS (familial advanced sleep phase syndrome) were reported: in one case, FASPS is associated with an amino acid mutation of a phosphorylatable residue of *hPer2* (36), while in the other, the syndrome is linked to a mutation of hCKI δ , by which the PER-phosphorylating activity is increased (9, 41). In addition, delayed sleep phase syndrome has been reported to associate with a missense mutation of CKI ϵ (35).

Compared to PER proteins having modest inhibitory effects on CLOCK-BMAL1-mediated transcriptional activation, CRY proteins inhibit the transactivation far more strongly (22). Mammals have two homologous *Cry* genes, *Cry1* and *Cry2*. Mice deficient in both *Cry* genes exhibit arrhythmic behavior immediately after being placed in constant darkness (37), indicating their critical role(s) in generating the circadian rhythm in mammals. Importantly, mutant mice deficient in individual *Cry* genes show distinct phenotypes; *Cry1* and *Cry2* knockout mice display an about 1-h-shorter and -longer free-running period, respectively (37, 39). This observation raised an as yet uncharacterized mechanism in which CRY1 and CRY2 distinguishably contribute to the clockwork, although their amino acid sequences are highly similar to each other except for their very unique C-terminal tails. It has been recently shown that an F-box protein, Fbxl3, mediates proteasomal degradation of both the CRY1 and CRY2 proteins to regulate the period length of circadian clock oscillation (4, 12, 32). On the other hand, we previously found a CRY2-specific degradation pathway sensitive to MG132, a 26S proteasome inhibitor (16). This

* Corresponding author. Mailing address: Department of Biophysics and Biochemistry, Graduate School of Science, University of Tokyo, Hongo 7-3-1, Bunkyo-Ku, Tokyo 113-0033, Japan. Phone: 81-3-5841-4381. Fax: 81-3-5802-8871. E-mail: sfukada@mail.ecc.u-tokyo.ac.jp.

[†] Present address: University of California, San Diego, Cell and Developmental Biology, 9500 Gilman Drive no. 0116, La Jolla, CA 92093-0116.

[‡] Present address: Molecular Genetics Research Laboratory, Graduate School of Science, University of Tokyo, Hongo 7-3-1, Bunkyo-ku, Tokyo 113-0033, Japan.

§ Supplemental material for this article may be found at <http://mcb.asm.org/>.

[∇] Published ahead of print on 1 February 2010.

pathway depends on CRY2 phosphorylation by GSK-3 β (glycogen synthase kinase 3 β) at Ser553, which lies in the C-terminal tail, unique to CRY2. In general, GSK-3 β phosphorylates Ser/Thr residues of substrates in a manner dependent on prior phosphorylation of the Ser/Thr residue that is located four residues carboxyl-terminal to the target site (8). Therefore, a key enzyme in the degradation process unique to CRY2 is the protein kinase catalyzing its Ser557 phosphorylation.

In the present study, we found that DYRK1A (dual-specificity tyrosine-phosphorylated and regulated kinase 1A) catalyzes the priming phosphorylation of CRY2 at Ser557, which allows GSK-3 β to subsequently phosphorylate CRY2 at Ser553 for its proteasomal degradation. This degradative mechanism appears CRY2 specific, because the CRY1 protein level was mostly unaffected by DYRK1A. In the mouse liver, DYRK1A kinase activity toward Ser557 of CRY2 showed circadian variation, with its peak in the accumulating phase of the CRY2 protein. Importantly, *Dyrk1a* knockdown caused earlier accumulation of nuclear CRY2 and shortened the period of the cellular rhythm. This effect of *Dyrk1a* knockdown was phenocopied by expression of an S557A/S553A mutant of CRY2 in cultured cells. Collectively, the unique sequence of the C-terminal tail of CRY2 contributes to the maintenance of normal clock oscillation by receiving the degradation signal from two clock-regulated protein kinases, DYRK1A and GSK-3 β . DYRK1A may be one of the key enzymes that regulate CRY2 function in the molecular clockwork.

MATERIALS AND METHODS

Animals and tissue collection. Animal experiments were conducted in accordance with the guidelines of the University of Tokyo. C57BL/6J mice were housed at 23 \pm 1°C in cages with food and water available *ad libitum*, and they were entrained to 12-h light/12-h dark (LD) cycles for at least 10 days. The entrained animals were transferred to constant dark (DD) conditions and sacrificed at various time points under DD conditions, in which their eyes were enucleated under dim red light (>640 nm). Then, the tissues were dissected under room light and homogenized for "total protein" extraction with buffer A (20 mM Tris-HCl, 1% [vol/vol] Triton X-100, 10% [vol/vol] glycerol, 137 mM NaCl, 1 mM dithiothreitol [DTT], 2 mM EDTA, 50 mM NaF, 1 mM Na₃VO₄, 4 μ g/ml aprotinin, 4 μ g/ml leupeptin, and 1 mM phenylmethylsulfonyl fluoride [PMSF]; pH 8.0 at 4°C).

Plasmids. Mammalian expression vectors encoding Myc epitope-tagged mouse CRY proteins were described previously (28). For FLAG-His-CRY2, an oligonucleotide encoding FLAG and a His \times 8 epitope sequence was fused to the 5' end of full-length mouse CRY2 coding sequence and cloned into pcDNA 3.1 (Invitrogen). Ser-to-Ala mutations were introduced by using a site-directed mutagenesis kit (Stratagene). An expression vector for *Xenopus* GSK-3 β was a kind gift of Yukiko Gotoh (University of Tokyo). Expression vectors for GST (glutathione *S*-transferase)-tagged rat DYRK1A, GFP (green fluorescent protein)-tagged rat DYRK1A, and its kinase-dead (KD) form were kind gifts of Walter Becker (Medizinische Fakultät der RWTH, Aachen, Germany). For FLAG-Fbx3, an oligonucleotide encoding the FLAG epitope sequence was fused to the 5' end of full-length mouse Fbx3 cDNA and cloned into pcDNA 3.1. pEGFP-C1 (for GFP expression; Clontech) or pcDNA3.1/*myc*-His/lacZ (for β -galactosidase expression; Invitrogen) was used for the control of transfection. shRNAs (short hairpin RNAs) were designed by using siDirect (<http://design.RNAi.jp/>), a Web-based online software program, and the following sequences were used: *Dyrk1a* sh1 (5'-GAACU UAGUA UCAUU CACUG U-3'), *Dyrk1a* sh2 (5'-GAGCU AUGGA CGUUA AUUUG A-3'), and luciferase sh (5'-GAUUU CGAGU CGUCU UAAUG U-3'). A control short hairpin (sh) (5'-GCCAU UCCUC AUAUA CUAUA G-3') was designed to prevent complementation to any known mouse and rat genes. Oligonucleotides to express the shRNAs were inserted into the pSilencer3.1-H1 puro vector (Ambion).

Preparation of nuclear and cytosolic fractions. The nuclear and cytosolic fractions of the mouse liver and cultured cells were prepared as previously described (44).

DEAE column chromatography. The entrained animals were transferred to DD conditions, and then the nuclear and cytosolic fractions of the mouse liver were prepared from mice sacrificed at circadian time 6 (CT6) (9 mice) and CT18 (9 mice) in the second day of DD conditions. CT is used for representing biological time under the DD condition, in which CT0 corresponds to the lights-on time in the LD cycle. Equal protein amounts of the nuclear (19 mg each) or cytosolic (560 mg each) fractions isolated at CT6 and CT18 were mixed together, and the two fractions were separately centrifuged at 83,800 \times *g* at 4°C for 30 min. Each supernatant was applied onto a DEAE-Toyopearl 650S column (Tosoh) pre-equilibrated by buffer B (10 mM HEPES-NaOH, 1 mM EDTA, 1 mM DTT, 1 mM PMSF, 4 μ g/ml aprotinin, 4 μ g/ml leupeptin, 50 mM NaF, and 1 mM Na₃VO₄; pH 7.8 at 4°C). Proteins adsorbed to the column were eluted with a linear gradient of increasing NaCl concentration from 0 mM to 400 mM, and the eluate was collected in fractions of 5 ml each.

In vitro measurement of Ser557 kinase activity. An aliquot of the fractionated sample of the mouse liver was mixed in a reaction mixture (30 μ l, final volume) with 300 ng of GST-CRY2 (28) in buffer C (25 mM HEPES-NaOH, 10 mM MgCl₂, and 1 mM DTT; pH 7.5 at 4°C) containing 1 mM ATP. After incubation at 37°C for 15 to 60 min, the phosphorylation reaction was quenched by the addition of 10 μ l of Laemmli sample buffer. The quenched samples were subjected to immunoblotting with anti-pS557-CRY2 antibody. We verified that the phosphorylation reactions were proportional to the incubation time and the dose of the sample. In some experiments analyzed in Fig. 1B, one of the kinase inhibitors was added to the reaction mixture (with 1% dimethyl sulfoxide [DMSO], final concentration). All kinase inhibitors were purchased from Calbiochem. In experiments analyzed in Fig. 1C, 75 ng of purified GST-DYRK1A (see below) or 250 U of recombinant CK2 (New England Biolabs) was used as the enzyme source.

Purification of GST-DYRK1A. GST-DYRK1A was expressed in *Escherichia coli* strain BL21(DE3) cultured with 100 μ M isopropyl- β -D-thiogalactopyranoside at 37°C for 4 h. Expressed GST fusion DYRK1A protein was purified by using a glutathione-Sepharose column (Amersham Biosciences, Inc.) according to the manufacturer's protocol. Recombinant GST-DYRK1A was subjected to SDS-PAGE analysis with Coomassie brilliant blue staining, and the protein content was estimated by densitometry of band intensities in the SDS-PAGE gel in comparison with those of serial dilutions of bovine serum albumin (BSA) standards in the same gel.

Immunoblotting. Proteins separated by SDS-PAGE were transferred to polyvinylidene difluoride membranes (Millipore). The blots were blocked by 1% (wt/vol) skim milk or 3% (wt/vol) BSA in TBS (50 mM Tris-HCl, 140 mM NaCl, 1 mM MgCl₂; pH 7.4) at 37°C for 1 h and then incubated at 4°C overnight with a primary antibody in the blocking solution. Primary antibodies used were anti-pS557-CRY2 antibody (16), anti-CRY2 antibody (Alpha Diagnostic International Inc.), anti-DYRK1A antibody, anti-GFP antibody, anti-GST antibody, anti-Myc antibody, anti-Raf-1 antibody, anti-TBP (TATA-binding protein) antibody (Santa Cruz Biotechnology), anti- β -actin antibody, anti-FLAG antibody (Sigma Aldrich), anti-phospho-ERK (extracellular signal-regulated kinase) antibody (New England Biolabs), antiphosphoserine antibody, and antiphosphothreonine antibody (Zymed). The primary antibodies were detected by HRP (horseradish peroxidase)-conjugated anti-rabbit or anti-mouse IgG antibody (Kirkegaard and Perry Laboratories). The positive signals were visualized by an enhanced chemiluminescence detection system (PerkinElmer Life Sciences). When indicated, the blots were stripped according to the manufacturer's protocol and reprobed. The band intensities were quantified by densitometric scanning of the immunoblotted membrane using Image Gauge ver. 4.0 software (Fujifilm Science Lab). Quantitative performance was assessed by determining the band intensities of serial dilutions of control samples in the same membrane.

Cell culture, transfection, and immunoprecipitation. Cell culture and transfection were performed as previously described (44). Transfected cells were then cultured in DMEM (Dulbecco's modified Eagle medium) for 48 h and harvested. For inhibition of proteasomal protein degradation or protein synthesis, MG 132 (final concentration, 10 μ M; Calbiochem) or cycloheximide (final concentration, 100 μ M; Nakalai tesque) was added to the culture medium. The harvested cells were lysed in buffer A and subjected to immunoblot analyses. For immunoprecipitation, the lysate prepared from the cultured cells or the mouse liver was incubated with 1.0 μ g of a precipitating antibody at 4°C overnight, followed by incubation with 20 μ l of protein G-Sepharose at 4°C for 3 h. The beads were washed three times with buffer A and subjected to immunoblotting or kinase assay.

Generation of stable cell lines. Rat-1 cells were transfected with the plasmid encoding shRNA (control sh, *Dyrk1a* sh1, or *Dyrk1a* sh2) by using LipofectAMINE 2000 (Invitrogen), and 1 day after the transfection, stable cell lines were selected with 1.0 μ g/ml puromycin. On the other hand, NIH 3T3 cells were

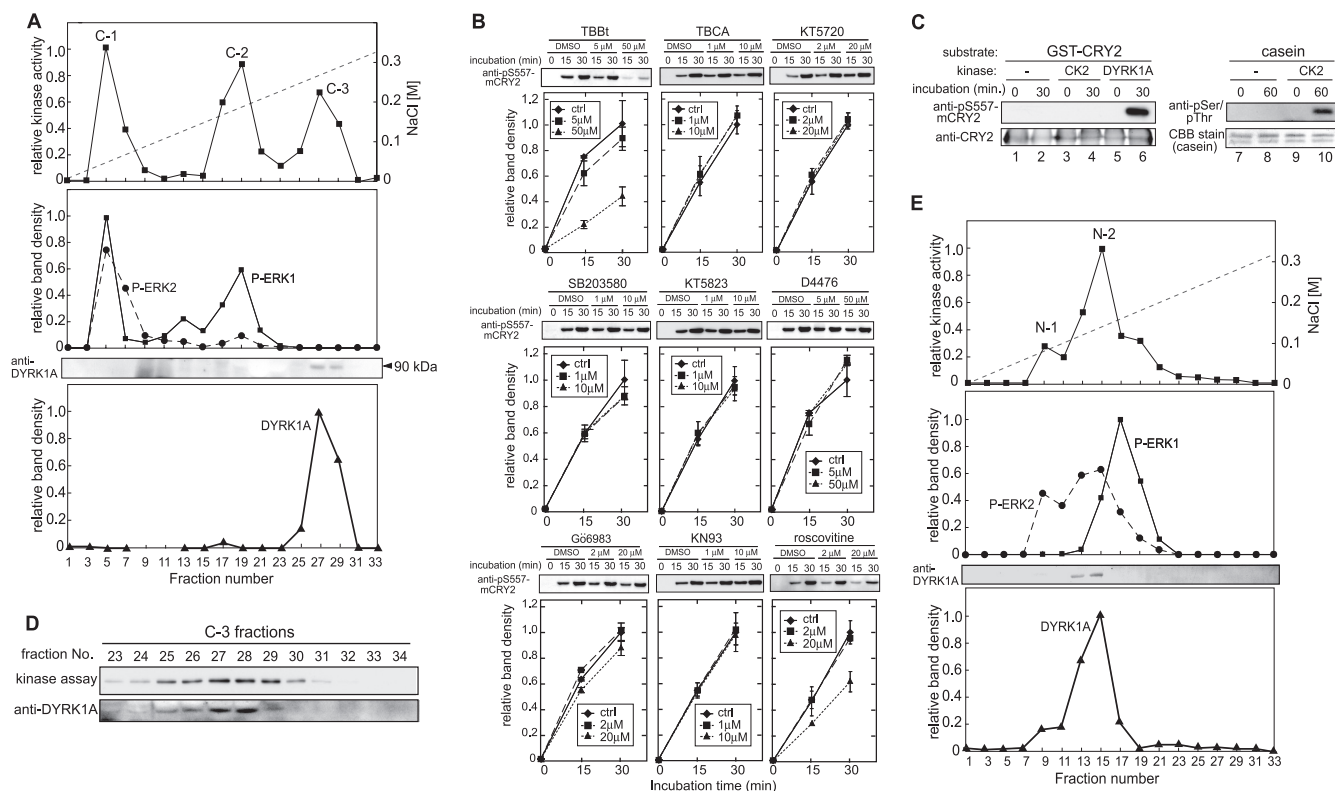


FIG. 1. Identification of Ser557 kinase *in vitro*. (A) The mixture of equal protein amounts of the cytosolic fraction of mouse liver isolated at CT6 and CT18 was separated on a DEAE-Sepharose column with a gradient of NaCl as indicated. Every other fraction was incubated with GST-CRY2 for 30 min, and the reaction mixture was immunoblotted with anti-pS557-CRY2 (top panel) and anti-phospho-ERK (second panel) antibodies. Each protein fraction was immunoblotted with anti-DYRK1A antibody (third and bottom panels). The intensity of the immunoreactive band was quantified and plotted by setting the highest value as 1. (B) An aliquot of fraction 27 was incubated with GST-CRY2 for the indicated time periods in the presence of various kinase inhibitors. The reaction mixtures were then subjected to immunoblotting with anti-pS557-CRY2 antibody (top panel), and normalized band intensities were plotted in the bottom panel (means \pm variation; $n = 2$). (C) Recombinant CK2 or GST-DYRK1A was incubated with GST-CRY2 (left panel) or CK2 was incubated with dephosphorylated casein (right panel) for indicated time periods. The reaction mixtures were subjected to immunoblotting or Coomassie brilliant blue (CBB) staining. (D) Aliquots of protein fractions 23 to 34 in the C-3 peak were incubated with GST-CRY2 for 30 min and immunoblotted with anti-pS557-CRY2 antibody (top panel). The same fractions were immunoblotted with anti-DYRK1A antibody (bottom panel). (E) The mixture of equal protein amounts of nuclear fraction of the mouse liver prepared at CT6 and CT18 was separated on a DEAE-Sepharose column with a gradient of NaCl as indicated. Each fraction was analyzed as for panel A.

transfected with the plasmid for FLAG-His-CRY2 by using LipofectAMINE PLUS (Invitrogen), and one day after the transfection, stable cell lines were selected with 3.0 mg/ml G418.

Sequential *in vitro* kinase assay. Myc-tagged CRY2 was expressed in HEK293T cells and immunoprecipitated with anti-Myc antibody. The beads were washed three times with buffer D (50 mM Tris-HCl, 0.1 mM EDTA, 5 mM DTT, 2 mM MnCl₂, and 0.01% Brij 35; pH 7.5), and the final suspension (30 μ l) was incubated with 200 U of lambda protein phosphatase (Sigma) at 30°C for 1 h. The beads were then washed three times with buffer C and incubated with 75 ng of GST-DYRK1A at 30°C for 30 min in 30 μ l of buffer C containing 1 mM ATP. The beads were washed three times with buffer C and incubated with 250 U of recombinant GSK-3 β (New England Biolabs) at 30°C for 30 min in 30 μ l of buffer C containing 1 mM ATP. The phosphorylation reaction was quenched by the addition of 10 μ l of Laemmli sample buffer.

Real-time monitoring of rhythmic gene expression. The luciferase reporter vector containing the 0.3-kb promoter region of the mouse *Bmal1* gene (*Bmal1*us0.3-luc) was described previously (21). Real-time monitoring of luciferase expression was performed as previously described (21). The period length was determined by calculating a mean period of the peak-to-peak and trough-to-trough duration between day 2 and day 4.

Staining of cultured cells. NIH 3T3 cells growing on chamber slides were transfected with Myc-CRY2 in combination with expression plasmid for shRNA. Forty-eight hours after transfection, they were fixed with 4% paraformaldehyde in PB (0.1 M sodium phosphate; pH 7.4 at 4°C), washed with TBS, and perme-

abilized with 0.1% (wt/vol) Triton X-100 in TBS (T-TBS) for 5 min at room temperature. After incubation with a blocking buffer (3% BSA in TBS) for 30 min at room temperature, the cells on the slide were incubated for 24 h at 4°C with anti-Myc antibody (Santa Cruz Biotechnology) in the blocking buffer. They were rinsed with TBS and then incubated for 2 h at room temperature with Alexa 568-conjugated anti-mouse IgG antibody (Molecular Probes). The cells were given a final wash with TBS, stained by DAPI (4',6-diamidino-2-phenylindole) for visualizing DNA, and mounted with an aliquot of antifade mounting medium (ProLong Gold; Invitrogen).

Competitive enzyme-linked immunosorbent assay (ELISA). Wells of 96-well microtiter plates were coated with 100 ng of Ser557-phosphorylated GST-CRY2 (28) dissolved in 100 μ l of TBS overnight at 4°C. After the wells were washed twice with 300 μ l of 3% (wt/vol) BSA-TBS, they were blocked with 3% (wt/vol) BSA-TBS for 1 h at 37°C. The primary antibody used was 100 μ l of anti-pS557-CRY2 antibody in the blocking solution (1:1,000 dilution) that had been preincubated with various concentrations of synthetic peptides overnight at 4°C. After incubation with the preincubated primary antibody for 1 h at 37°C, the wells were washed twice with the blocking solution. To the washed wells was added 100 μ l of 0.5 μ g/ml HRP-conjugated anti-rabbit IgG and incubated for 1 h at 37°C. After two washes with T-TBS and then two washes with TBS, the wells were filled with 100 μ l of 3,3',5,5'-tetramethylbenzidine solution (100 μ g/ml) dissolved in citrate phosphate buffer (pH 5.0) containing 0.006% of H₂O₂. After incubation for 5 min at room temperature, 100 μ l of 1 M H₂SO₄ was added to stop the enzyme reaction, and the difference absorbance between 492 nm and 620 nm of

TABLE 1. Subcellular distribution of Ser557 kinase activity and GSK-3 β protein in mouse liver

Fraction ^a (CT6 + CT18)	Relative Ser557 kinase activity ^b [per min · g tissue] (%)	Relative GSK-3 β immunoreactivity ^c [per g tissue] (%)
Nucleus	23 ± 5 (19)	5.3 ± 0.8 (5)
Cytosol	100 ± 12 (81)	100 ± 5 (95)

^a Each fraction is a mixture of equal protein amounts of those prepared at CT6 and -18.

^b The total kinase activity in the liver cytosol was set to 100. Values are means ± SEM ($n = 3$).

^c The immunoreactive bands detected by the immunoblotting analysis were quantified as described in Materials and Methods. The relative band intensities were shown by setting the value of the cytosol fraction to 100. Values are means ± SEM ($n = 3$).

each well was read on a microplate reader. The immunoreactivity of anti-pS557-CRY2 antibody toward a synthetic peptide that is doubly phosphorylated at Ser553 and Ser557 or a peptide singly phosphorylated at Ser557 was characterized by this experiment (see Fig. S1 in the supplemental material). We concluded that phosphorylation of Ser553 caused no significant loss of immunoreactivity of the antibody against pSer557-CRY2. The synthetic peptides used were as follows: non-P peptide (CSGPASP β PKR β KLE), pSer557 peptide (CSGPA[pS]PKR β KLE), and pS553/pS557 peptide (C[pS]GPA[pS]PKR β KLE).

Statistics. Where indicated, two experimental data sets were compared by using a two-tailed Student t test. Significance of circadian rhythmicity was analyzed by one-way ANOVA (analysis of variance). Two-way ANOVA was used to analyze the difference in circadian expression profiles of CRY2 between control and *Dyrk1a*-knocked-down Rat-1 cells.

RESULTS

Identification of Ser557 kinase of CRY2. We previously found that CRY2 is phosphorylated at Ser557 by ERK1 (extracellular signal-regulated protein kinase 1) and ERK2 *in vitro* (28). However, neither activation nor inhibition of the ERK pathway altered the phosphorylation state of CRY2 at Ser557 in cultured cells (16), indicating that a protein kinase(s) other than ERK contributes to Ser557 phosphorylation of CRY2 *in vivo*. To search for the protein kinase (Ser557 kinase), we first examined subcellular localization of Ser557-phosphorylating enzyme activity, which can be quantitated by a biochemical assay with an antibody specific to the Ser557-phosphorylated form of CRY2 (16) in combination with a recombinant substrate, GST-CRY2 (see Materials and Methods). By using this *in vitro* kinase assay, we found that the Ser557 kinase activities were distributed between the nuclear and cytosolic fractions prepared from mouse liver, where the cytosolic fraction retained a larger proportion (81%) of the activities (Table 1). Then, the cytosolic fraction was subjected to DEAE column chromatography, which developed three peaks of Ser557 kinase activity, designated C-1, C-2, and C-3 (Fig. 1A, top panel). The immunoblot analysis of the fractions with an antibody specific to phosphorylated (activated) ERKs demonstrated that the activity peaks of C-1 and C-2 paralleled the elution of activated ERK1 and ERK2, whereas the C-3 fractions were devoid of activated ERK1 and ERK2 (Fig. 1A, top and middle panels).

The Ser557 kinase activity in the C-3 peak fraction was characterized by performing the *in vitro* kinase assay in the presence of various kinase inhibitors. Many drugs, including D4476 (a CKI inhibitor), SB203580 (a p38 inhibitor), KT5720

(a PKA [cAMP-dependent protein kinase] inhibitor), Gö6983 (a protein kinase C [PKC] inhibitor), KT5823 (a PKG [cGMP-dependent protein kinase] inhibitor), and KN93 (a calcium/calmodulin-dependent protein kinase II [CaMKII] inhibitor), had no significant inhibitory effect on the Ser557 kinase activity (Fig. 1B). A marked inhibition was observed with 4,5,6,7-tetrabromobenzotriazole (TBBt) (Fig. 1B), a drug that inhibits CK2 and DYRK1A (29), while the Ser557 kinase activity was not affected by tetrabromocinnamic acid (TBICA) (Fig. 1B), which inhibits CK2 but not DYRK1A activity (26), highlighting the role of DYRK1A as a potential Ser557 kinase.

We found that recombinant GST-DYRK1A (see Materials and Methods) phosphorylates GST-CRY2 at Ser557 (Fig. 1C, lane 6). In contrast, recombinant CK2 was unable to catalyze Ser557 phosphorylation (lane 4) under the conditions where it phosphorylates casein (lanes 9 and 10). An immunoreactive band with a molecular mass close to that of DYRK1A (calc. 86 kDa) was detected in C-3 fractions (Fig. 1A, third and bottom panels), and the elution profile of DYRK1A immunoreactivities closely matched that of the Ser557 kinase activities (Fig. 1D). In parallel DEAE column chromatography of the nuclear fraction, the overall elution profile of Ser557 kinase activity mirrored that of the DYRK1A-immunoreactive band (Fig. 1E). These results raised DYRK1A as a potential kinase catalyzing Ser557 phosphorylation, and it fell in line with the fact that DYRK1A is a proline-directed Ser/Thr kinase (18).

DYRK1A is responsible for Ser557 phosphorylation of CRY2. DYRK1A is a member of the DYRK family of protein kinases, and the members are distantly related to ERKs and CDKs (cyclin-dependent protein kinases) in amino acid sequences (17). Mammalian DYRK1A is expressed ubiquitously in adult and fetal tissues (13, 25) and also in NIH 3T3 cells (Fig. 2A), a cell model that is widely used for studies of peripheral clocks operating in a wide range of tissues (43). Because transfected Myc-CRY2 was phosphorylated at Ser557 by an enzyme activity intrinsic to NIH 3T3 cells (Fig. 2G, lane 1), we asked whether DYRK1A is responsible for the phosphorylation. We found that the Ser557-phosphorylating activity intrinsic to NIH 3T3 cells was markedly attenuated by shRNAs against *Dyrk1a*, sh1 or sh2 (Fig. 2D), which reduced the expression of not only cotransfected GFP-DYRK1A (Fig. 2B) but also endogenous DYRK1A in NIH 3T3 cells (Fig. 2C). It should be noted that this analysis was performed in the presence of a proteasome inhibitor, MG132, which prevents CRY2 from Ser557 phosphorylation-dependent degradation (see below). Under this condition, the knockdown of *Dyrk1a* had a marginal effect on the cellular localization of Myc-CRY2 (Fig. 2E and F), indicating that the shRNA-mediated downregulation of Ser557 phosphorylation is not due to altered subcellular localization of CRY2. These observations demonstrate that DYRK1A phosphorylates CRY2 at Ser557 in NIH 3T3 cells.

This conclusion was also supported by a gain-of-function study of DYRK1A: coexpression of wild-type (WT) DYRK1A with Myc-CRY2 in NIH 3T3 cells (Fig. 2G, lane 2) remarkably stimulated Ser557 phosphorylation of Myc-CRY2 (top panel), yielding its upshifted and supershifted bands (open and gray arrowheads, respectively), whereas coexpression of a kinase-dead (KD) form of DYRK1A did not produce these extra bands (lane 3). In a similar experiment (Fig. 2H), S557A mutation of CRY2 abrogated the electrophoretic retardation of

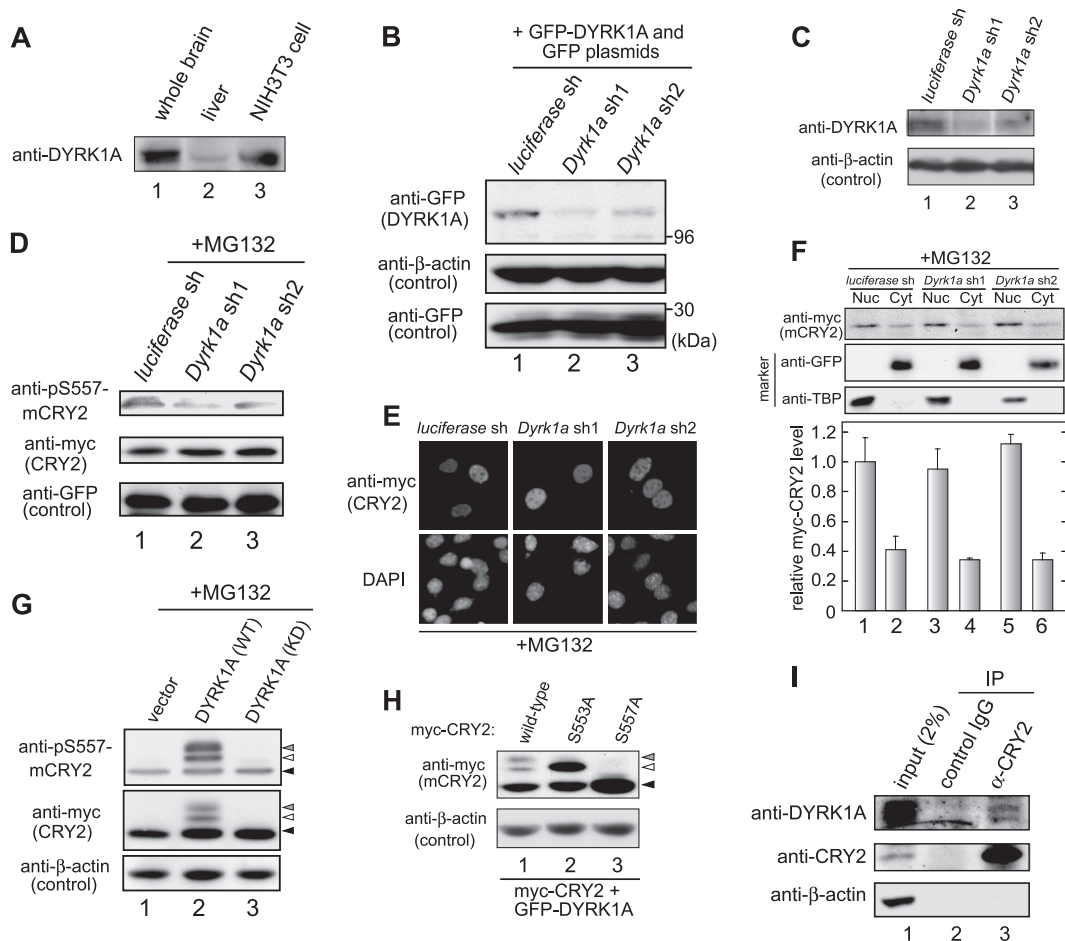


FIG. 2. Phosphorylation of CRY2 at Ser557 by DYRK1A. (A) The lysates of mouse whole brain, liver, and unsynchronized NIH 3T3 cells (30 μ g protein for each lane) were subjected to immunoblotting with anti-DYRK1A antibody. The lysate of whole brain and liver were prepared from entrained mice at CT18. (B) NIH 3T3 cells were transfected with an expression plasmid for GFP-DYRK1A and GFP in combination with a *Dyrk1a* shRNA or *luciferase* shRNA expression plasmid. GFP was simultaneously expressed to examine the specificity of shRNA. The cell lysates were subjected to immunoblotting. GFP served as a transfection control (bottom panel). (C) NIH 3T3 cells were transiently transfected with a plasmid encoding *Dyrk1a* shRNA or *luciferase* shRNA, and the transfected cells were selected in medium containing 1.0 μ g/ml puromycin. The lysates of the puromycin-resistant cells were subjected to immunoblotting. β -Actin served as a loading control (bottom panel). (D) NIH 3T3 cells were transfected with Myc-CRY2 in combination with either shRNA for *luciferase* or *Dyrk1a*. The cell lysates were subjected to immunoblotting. GFP served as a transfection control (bottom panel). (E) NIH 3T3 cells were transfected with Myc-CRY2 in combination with either shRNA for *luciferase* or *Dyrk1a*, and then the cells were immunostained with anti-Myc antibody (top panel). Cell nuclei were stained by DAPI (bottom panel). (F) Under the same conditions as for panel E, the nuclear and cytosolic fractions were prepared from the cells (300 μ l for each fraction). Equal volumes (30 μ l) of nuclear or cytosolic fractions of the cells were subjected to immunoblotting. Immunoblotting with anti-GFP (second panel) and anti-TBP antibody (third panel) verified separation of the nuclear and cytosolic proteins. The intensity of the immunoreactive band of Myc-CRY2 was quantified and is shown as values relative (means with SEM; $n = 3$) to that of the nuclear fraction of the cells transfected with shRNA for *luciferase* (bottom panel). (G) NIH 3T3 cells were transiently transfected with expression plasmids for Myc-CRY2 and GFP-DYRK1A. The cell lysates were subjected to immunoblotting. β -Actin served as a loading control (bottom panel). Upshifted and supershifted bands of CRY2 were indicated by open and gray arrowheads, respectively. (H) NIH 3T3 cells were transiently transfected with expression plasmids for GFP-DYRK1A and wild-type Myc-CRY2 or its SA mutant (S553A or S557A). The cell lysates were subjected to immunoblotting. β -Actin served as a loading control (bottom panel). (I) The whole-brain lysate prepared at CT18 was immunoprecipitated by using anti-CRY2 antibody, and then immunoprecipitates were subjected to immunoblotting. Normal rabbit IgG was used instead of anti-CRY2 antibody as a control. In panels D, E, F, G, and H, cells were treated with MG132 for 8 h before harvesting to inhibit proteasomal degradation of Ser557-phosphorylated CRY2.

the protein band (lanes 1 and 3), indicating that phosphorylation of Ser557 triggers the subsequent phosphorylation that causes the upshift and supershift of CRY2 bands. We previously demonstrated that the CRY2 protein band is upshifted by its secondary phosphorylation at Ser553 and that the mutation of Ser553 to Ala (S553A) abrogates GSK-3 β -dependent upshift of the protein band (16). In the presence of overexpressed DYRK1A, however, the S553A mutation of CRY2 did

not prevent the upshift of the protein band (lane 2), suggesting that overexpression of DYRK1A in cells may stimulate phosphorylation of an additional site(s) that causes the supershift of wild-type CRY2 as well as the upshift of S553A-CRY2.

The results of experiments carried out *in vitro* (Fig. 1C) and with NIH 3T3 cells (Fig. 2D) strongly suggest that DYRK1A directly phosphorylates CRY2 at Ser557. Then, we examined *in vivo* interaction between CRY2 and DYRK1A in lysates

from the mouse whole brain, in which the DYRK1A protein level is relatively high among the tissues (Fig. 2A). Coimmunoprecipitation of DYRK1A with anti-CRY2 antibody (Fig. 2I) demonstrated their physical interaction in the brain and suggests a functional coupling of CRY2 and DYRK1A *in vivo*.

DYRK1A primes for GSK-3 β phosphorylation of CRY2. We investigated the potential role of DYRK1A as the priming kinase of CRY2 in a sequential *in vitro* kinase assay (see Materials and Methods). Ser557 phosphorylation of Myc-CRY2 was observed by incubation with recombinant GST-DYRK1A (Fig. 3A, lane 2). The subsequent incubation with recombinant GSK-3 β caused accumulation of the upshifted band of Myc-CRY2 in addition to the original band, both in the Ser557-phosphorylated form (lane 4, open and solid arrowheads, respectively). The formation of the upshifted band was absolutely dependent on the primary incubation with DYRK1A (lane 3). The mutation of Ser557 to Ala completely abolished the mobility shift of the Myc-CRY2 protein band (lanes 5 to 8). On the other hand, the mutation of Ser553 to Ala had no significant effect on primary phosphorylation at Ser557 by DYRK1A but abrogated upshift of the protein band (lanes 9 to 12), confirming that the upshifted band represents Ser557/Ser553-dually phosphorylated CRY2. We next examined the effect of *Dyrk1a* knockdown on the sequential phosphorylation of CRY2 in NIH 3T3 cells, in which CRY2 Ser557 is phosphorylated by endogenous DYRK1A activity (Fig. 2G, lane 1). In the presence of MG132 in culture, coexpression of GSK-3 β with Myc-CRY2 resulted in accumulation of the upshifted band (Fig. 3B, lane 2, open arrowhead). Cotransfection of the shRNA toward *Dyrk1a*, sh1 or sh2, suppressed the formation of the upshifted band of dually phosphorylated CRY2 (lanes 3 and 4). Collectively, these observations indicate that DYRK1A-catalyzed priming phosphorylation of CRY2 at Ser557 plays a key role for subsequent (secondary) GSK-3 β -catalyzed Ser553 phosphorylation.

Sequential phosphorylation by DYRK1A and GSK-3 β regulates the protein level of CRY2. The biological significance of the sequential phosphorylation of CRY2 was studied by coexpression of DYRK1A and GSK-3 β in NIH 3T3 cells. Apparently these two kinases additively downregulated the protein level of Myc-CRY2 (Fig. 3C, lanes 1 to 4). As described, endogenous DYRK1A activity should contribute to the decrease of the Myc-CRY2 protein in GSK-3 β -transfected cells (lane 3). A similar decrease of the Myc-CRY2 protein in DYRK1A-transfected cells (lane 2) suggests that GSK-3 β may also be expressed in NIH 3T3 cells, although the activity should not be so high as to cause the upshift of the CRY2 band (Fig. 3B, lane 1). On the other hand, the protein level of not only the S557A mutant but also the S553A mutant of Myc-CRY2 was insensitive to expression of DYRK1A and/or GSK-3 β (Fig. 3C, lanes 5 to 12). In contrast, DYRK1A had no significant effect on the protein level of Myc-CRY1, while GSK-3 β slightly downregulated the Myc-CRY1 level (Fig. 3D). This observation suggests that DYRK1A triggers the degradation mechanism specific to CRY2. We next examined the effect of *Dyrk1a* knockdown on the CRY2 protein level by transfecting shRNA toward *Dyrk1a*, sh1 or sh2. In both cases, the protein levels of cotransfected Myc-CRY2 were significantly elevated compared to the control level with *luciferase* shRNA (Fig. 3E, lanes 1 to 3). On the other hand, the protein level of the S557A

mutant of Myc-CRY2 expressed in NIH 3T3 cells (lane 4) was about 2-fold higher than that of wild-type Myc-CRY2 (lane 1), and importantly, the stabilizing effect of *Dyrk1a* knockdown was no longer observed (lanes 4 to 6). These results indicate that DYRK1A cooperates with GSK-3 β to regulate the CRY2 protein level in NIH 3T3 cells.

Circadian variation of DYRK1A activity *in vivo*. In the mouse liver, the protein level of DYRK1A showed a circadian change, peaking at CT18 (Fig. 4A, bottom panel, circles) ($P < 0.05$ by one-way ANOVA). We then examined a temporal variation of DYRK1A activity toward CRY2 by performing an immune complex assay-based Ser557 kinase assay. The assay was validated by the fact that DYRK1A immunoprecipitates prepared from liver lysate at CT18 displayed Ser557-phosphorylating activity toward GST-CRY2 while control IgG precipitated no such activity (Fig. 4B). In addition, treatment of DYRK1A immunoprecipitates with 50 μ M TBBt attenuated the activity (Fig. 4C). Under this condition, the Ser557-phosphorylating activity of DYRK1A of the liver lysate showed a circadian variation with a peak at CT18 (Fig. 4A, bar graph) ($P < 0.05$ by one-way ANOVA), a temporal profile that is very similar to that of DYRK1A protein fluctuation (circles). The peak of DYRK1A activity was slightly early shifted from that of Ser557-phosphorylated CRY2, whose level peaked late at night (CT22), which also paralleled that of CRY2 protein accumulation (Fig. 4A, third panel). Because DYRK1A activity reaches its peak and trough when CRY2 protein levels are in the middle of the increasing and decreasing phases, respectively, it is predicted that DYRK1A plays a more active role in regulation of the process of CRY2 accumulation rather than a role in its decline process (see Discussion; see also Fig. 6D). A similar circadian variation in the DYRK1A protein level was observed in the mouse whole brain lysate (see Fig. S2 in the supplemental material).

DYRK1A regulates circadian accumulation of CRY2 and the period of circadian rhythm. We asked whether DYRK1A plays a role in oscillation of the cellular clock. Cultured NIH 3T3 cells were transiently transfected with a luciferase reporter that is driven by the 0.3-kb promoter region of the mouse *Bmal1* gene (*Bmal1*us0.3-luc), and cellular bioluminescence signals were recorded continuously after synchronization of the cellular clocks by a dexamethasone pulse. The signals recorded from the cells cotransfected with a control GFP expression vector showed circadian rhythms with a period of 20.78 ± 0.22 h (Fig. 5A and E). When parallel cultures were cotransfected with GFP-DYRK1A (WT), the period of the cellular rhythm was significantly lengthened, to 21.61 ± 0.07 h (Fig. 5A and E). In Rat-1 cell lines stably expressing *Dyrk1a* shRNA (sh1 or sh2), on the other hand, the DYRK1A protein was downregulated and the Ser557 phosphorylation level of CRY2 was reduced in the presence of MG132 (Fig. 5B). In addition, we verified that *Dyrk1a* knockdown in sh1-expressing cells attenuated the degradation rate of endogenous CRY2 (Fig. 5C). Then, we examined the cellular rhythms in *Dyrk1a*-knocked-down cells. When sh1- or sh2-expressing cells were transfected with the *Bmal1*us0.3-luc reporter, a dexamethasone pulse induced bioluminescence rhythms with a period length of 21.81 ± 0.04 h or 21.80 ± 0.03 h, respectively, both of which were significantly shorter than the period of a control cell line, 22.26 ± 0.17 h (Fig. 5D and E).

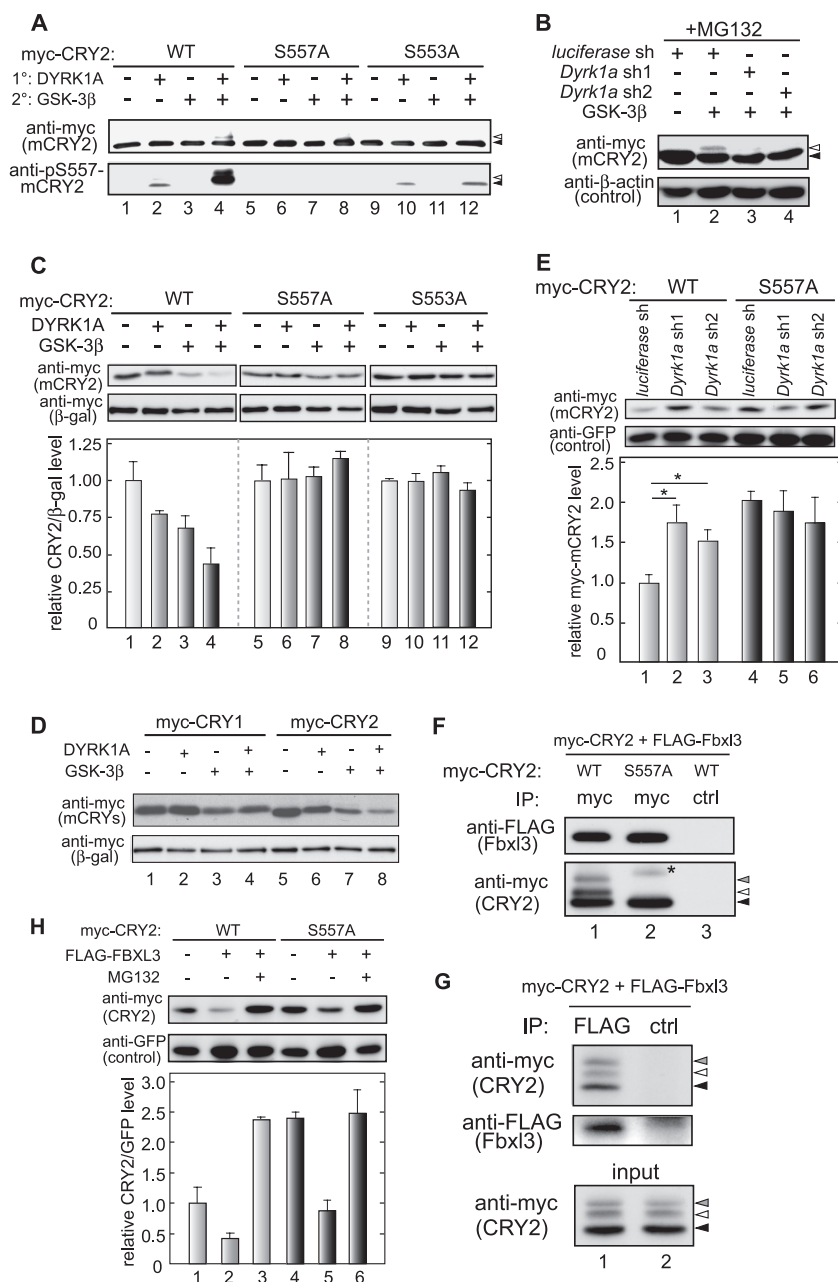


FIG. 3. Regulation of CRY2 protein level by DYRK1A- and GSK-3 β -mediated phosphorylation at Ser557 and Ser553. (A) the wild type (lanes 1 to 4), S557A mutant (lanes 5 to 8), or S553A mutant (lanes 9 to 12) of Myc-CRY2 expressed in HEK293T cells was subjected to a sequential *in vitro* kinase assay (see Materials and Methods). Then, reaction mixtures were analyzed by immunoblotting. (B) NIH 3T3 cells were transfected with a plasmid for Myc-CRY2 in combination with the *Dyrk1a* shRNA or GSK-3 β expression construct. The cells were treated with MG132, and the resultant cells were subjected to immunoblotting. (C) NIH 3T3 cells were transfected with plasmids for Myc-CRY2 (WT, lanes 1 to 4; S557A, lanes 5 to 8; S553A, lanes 9 to 12) in combination with the DYRK1A and/or GSK-3 β expression construct. The cell lysates were subjected to immunoblotting (top and middle panels). The quantified intensity was plotted in the bottom panel (means with SEM, $n = 3$) by setting the mean of control cells (lanes 1, 5, and 9) to 1. (D) NIH 3T3 cells were transiently transfected with either the Myc-CRY1 or Myc-CRY2 expression plasmid in combination with plasmids for GFP-DYRK1A and GSK-3 β . The cell lysates were subjected to immunoblotting. (E) NIH 3T3 cells were transfected with Myc-CRY2 (WT, lanes 1 to 3; S557A mutant, lanes 4 to 6) in combination with *Dyrk1a* shRNA constructs. The cell lysates were subjected to immunoblotting (top and middle panels). The quantified intensity was plotted in the bottom panel (means with SEM; $n = 4$) by setting the means of the control cells (lanes 1) to 1 (bottom panel). A single asterisk indicates a P value of 0.05 (by two-tailed Student t test). (F and G) NIH 3T3 cells were transiently transfected with the wild type or S557A mutant of the Myc-CRY2 expression plasmid and plasmids for FLAG-Fbxl3, GFP-DYRK1A, and GSK-3 β (F) or transfected with wild-type Myc-CRY2 expression plasmid and plasmids for FLAG-Fbxl3, GFP-DYRK1A, and GSK-3 β (G). The cells were treated with MG132 for 8 h, and the cell lysates were subjected to immunoprecipitation with anti-Myc antibody (F) and anti-FLAG antibody (G). Normal mouse IgG was used as a control. The cell lysates and immunoprecipitants were subjected to immunoblotting. A nonspecific band is indicated by an asterisk. (H) NIH 3T3 cells were transiently transfected with the wild-type or S557A mutant Myc-CRY2 expression plasmid and plasmids for FLAG-Fbxl3. When indicated, the cells were treated with MG132 for 8 h. The cell lysates were subjected to immunoblotting (top and middle panels). Quantified intensities are plotted in the bottom panel (means with SEM; $n = 3$) by setting the means of the control cells (lanes 1) to 1 (bottom panel).

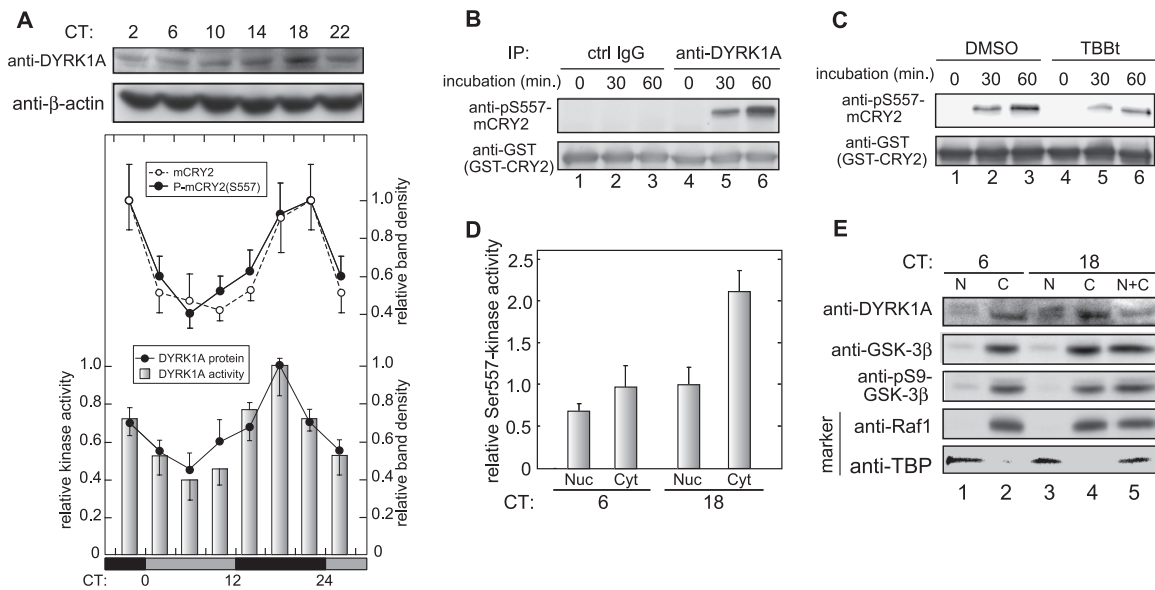


FIG. 4. Circadian rhythm of DYRK1A activity toward CRY2 in the mouse liver. (A) Total liver lysate prepared at various time points (CT2, -6, -10, -14, -18, and -22) were immunoblotted with anti-DYRK1A (top panel) and β -actin antibody (middle panel). For measurement of Ser557 kinase activity of DYRK1A, the protein was immunoprecipitated from mouse liver lysate (1 mg protein) with anti-DYRK1A antibody. The immunoprecipitate was then incubated with GST-CRY2 at 37°C for 30 min, and the reaction mixture was subjected to immunoblotting with anti-pS557-CRY2 and anti-CRY2 antibody. CRY2 was immunoprecipitated from the liver lysate with anti-CRY2 antibody and immunoblotted with anti-pS557-CRY2 and anti-CRY2 antibody. Quantified intensities were plotted in the third and bottom panels (means with SEM, $n = 4$ for DYRK1A and $n = 3$ for Ser557 kinase activity of DYRK1A, CRY2, and Ser557-phosphorylated CRY2) by setting the peak value to 1. The data for CT2 and -22 were double plotted. (B) The total lysate of the mouse liver (1 mg protein) prepared at CT18 was immunoprecipitated with normal rabbit IgG or anti-DYRK1A antibody, and the immunoprecipitate was incubated with GST-CRY2 at 37°C for indicated time periods. The reaction mixtures were subjected to immunoblotting. (C) The total lysate of the mouse liver (1 mg protein) prepared at CT18 was immunoprecipitated with anti-DYRK1A antibody. Then, the immunoprecipitate was incubated with GST-CRY2 at 37°C for indicated time periods in the presence or absence of TBBt (final concentration, 50 μ M). The reaction mixtures were subjected to immunoblotting. (D) Equal volumes of the nuclear and cytosolic fractions were prepared from mouse liver at CT6 and -18 (see Materials and Methods). Seventy-five μ l of nuclear or cytosolic fractions were immunoprecipitated with anti-DYRK1A antibody, and the immunoprecipitate was subjected to a Ser557 kinase assay. The activities were shown as values relative (means with SEM; $n = 3$) to that of the nuclear fraction at CT18. (E) Equal volumes (4 μ l) of these two fractions, prepared as for panel D, were immunoblotted with the indicated antibodies. Immunoblotting with anti-Raf-1 (fourth panel) and anti-TBP antibody (bottom panel) verified separation of the nuclear and cytosolic proteins.

The molecular basis for the period-shortening effect mediated by *Dyrk1a* knockdown was investigated by tracing the circadian profiles of CRY2 protein distribution in the cytosol and nuclei of *Dyrk1a* sh1-expressing Rat-1 cells. We found that after synchronization of the cellular clock, cytosolic CRY2 protein levels showed circadian variation at markedly higher levels compared to those observed for control shRNA-expressing cells (Fig. 5F, upper panel) ($P < 0.01$ by two-way ANOVA). In contrast, *Dyrk1a* knockdown had no significant effect on the peak and trough levels of nuclear CRY2 (bottom panel). These results highlight the cytosol as the major site for degradation of Ser557-phosphorylated CRY2. Importantly, *Dyrk1a* knockdown accelerated the timing of nuclear accumulation of CRY2 (bottom panel), probably in consequence of the elevation of cytosolic CRY2 (upper panel). A detailed time course examination during 26 to 38 h (second cycle) after the synchronization revealed a 2- to 4-h advance of the timing of the nuclear CRY2 accumulation (bottom panel, inset). These observations demonstrate pivotal roles of DYRK1A in not only regulating the protein levels of cytosolic CRY2 but also determining the timing of nuclear accumulation of CRY2.

S557A/S553A mutation of CRY2 phenocopies the effect of *Dyrk1a* knockdown. Finally, we examined whether a phos-

phorylation defect of CRY2 at Ser557/Ser553 may cause the short periods, which we observe in cells with reduced DYRK1A levels (Fig. 5). For this purpose, NIH 3T3 cell lines stably expressing FLAG-His-CRY2 (WT) or FLAG-His-CRY2 (S557A/S553A) were generated, and we selected cell populations in which the expression level of exogenously expressed CRY2 was comparable to that of endogenous CRY2 (Fig. 6A). A potential difference in clonal variability with regard to circadian dynamics was eliminated by using pools of the subcloned cells. These cells were transiently transfected with the *Bmal1*us0.3-luc reporter. We found that the cells expressing S557A/S553A mutant FLAG-His-CRY2 showed circadian rhythms with a period of 22.18 ± 0.06 h, and this period was significantly shorter than that of the cells expressing wild-type FLAG-His-CRY2, 22.73 ± 0.09 h (Fig. 6B and C). It is most probable that phosphorylation of CRY2 at Ser557/Ser553 is required for the circadian time-keeping mechanism.

DISCUSSION

DYRK1A, a member of the DYRK family, is expressed ubiquitously in mammalian tissues (13, 25), with high expression levels in the brain during development (25). As with

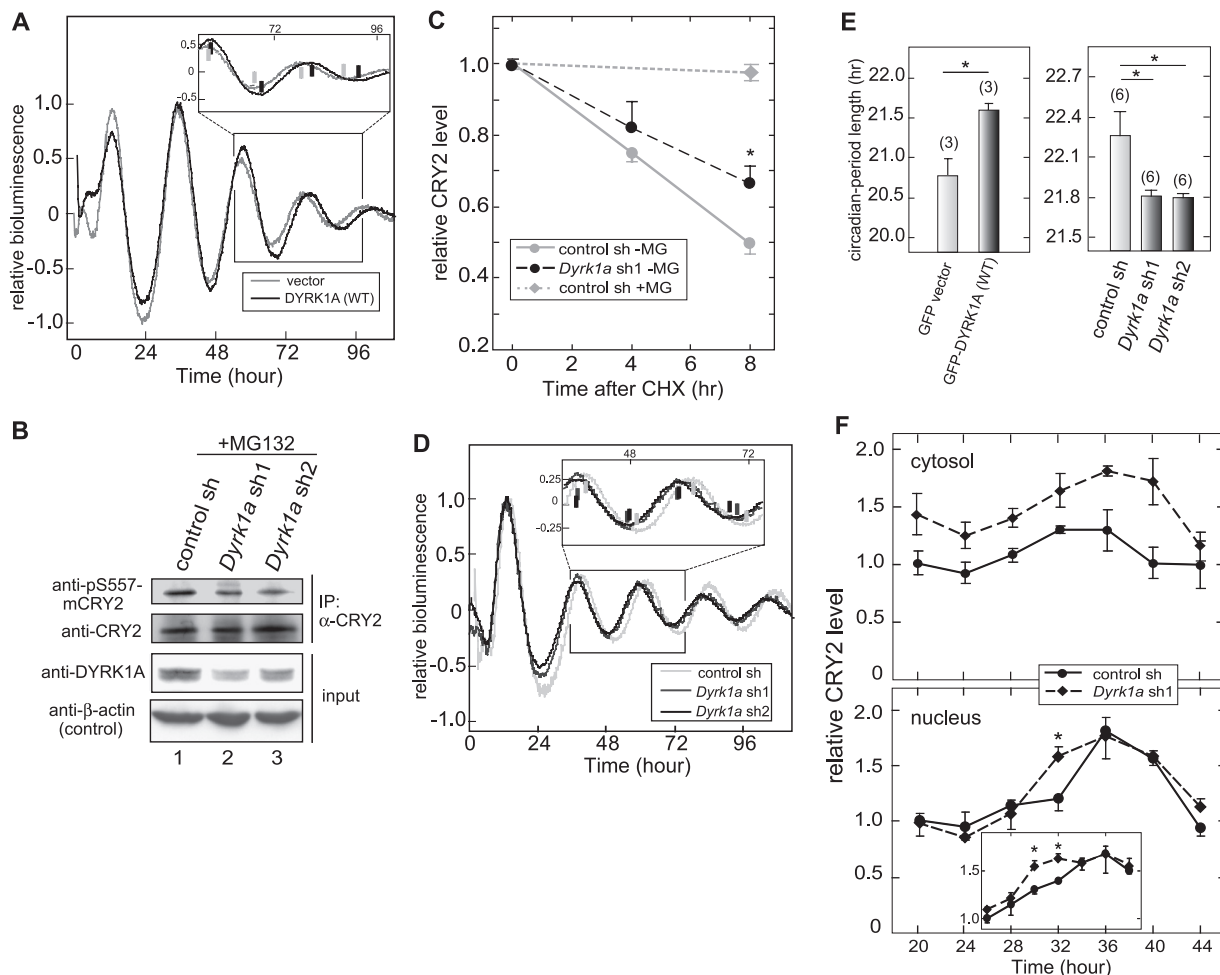


FIG. 5. Alteration of the accumulation profile of CRY2 and the period length of the bioluminescence rhythms by knockdown of *Dyrk1a* in cultured cells. (A) NIH 3T3 cells were transiently transfected with a DYRK1A expression plasmid and *Bmal1*-luciferase reporter. A representative set of bioluminescence rhythms is shown. (B) Twenty-four hours after plating of Rat-1 stable cell lines, the cells were cultured in 10 μ M MG132 for 12 h, and total lysates of the cells were immunoblotted with anti-DYRK1A (third panel) and β -actin antibody (bottom panel). For the detection of the Ser557-phosphorylated form of CRY2, the protein was immunoprecipitated from the lysate with anti-CRY2 antibody and immunoblotted with anti-pS557-CRY2 antibody (top panel) and anti-CRY2 antibody (second panel). (C) Rat-1 cells stably expressing control sh or *Dyrk1a* sh1 were plated 24 h before the experiment and synchronized by 2-h pulse treatment with dexamethasone. Twenty-four hours after the synchronization, the cells were incubated in the presence of cycloheximide at a final concentration of 100 μ M for the indicated time periods. Then, the cells were harvested, and the total lysates of the cells were immunoblotted with anti-CRY2 antibody. Quantified intensities were plotted (means with SEM; $n = 3$) by setting the peak value to 1. A single asterisk indicates a P value of 0.05 versus results for cells stably expressing control shRNA in the absence of MG132 (by two-tailed Student's t test). (D) Rat-1 fibroblasts stably expressing *Dyrk1a* shRNA were transiently transfected with *Bmal1*-luciferase reporter. Twenty-four hours after transfection, the cells were synchronized with dexamethasone treatment for 2 h, and luciferase activity was monitored. The period length of bioluminescence rhythm in panels A and D is shown in panel E. Data are means with SEM, and the number of independent samples is indicated in parentheses. A single asterisk indicates a P value of 0.05 (by two-tailed Student's t test). (F) Rat-1 cells stably expressing control shRNA or *Dyrk1a* shRNA sh1 were synchronized with dexamethasone treatment. The cytosol and nuclear fractions of the cells were collected at 4-h or 2-h (inset) intervals. These fractions were immunoblotted with anti-CRY2 antibody, and the band intensities were quantified. Data are means with SEM ($n = 3$), and the value of control cells at 20 h or 26 h (inset) was set to 1. A single asterisk indicates a P value of 0.05 versus results for cells stably expressing control shRNA (by two-tailed Student's t test).

CRY2, certain substrates of DYRK1A are targets for multi-step phosphorylation: priming phosphorylation of NFAT (nuclear factor of activated T cells) catalyzed by DYRK1A causes secondary phosphorylation catalyzed by GSK-3 or CKI, leading to NFAT inactivation to block NFAT-regulated gene expression (2, 14). *Dyrk1a* null mutant mice display a developmental delay and die during the period of organogenesis (7), revealing that DYRK1A is a regulator of body growth. In spite of the progress in understanding DYRK1A function, the substrates and physiological roles of DYRK1A other than in the

developmental system are poorly understood. Here we demonstrate that DYRK1A is an enzyme responsible for CRY2 Ser557 phosphorylation, which plays a critical role in regulating the protein level of CRY2 for normal oscillation of the circadian clock. The present study also sheds light on the molecular mechanism of how multiple protein kinases cooperate in molecular clockwork, because this represents the first example of a mammalian clock protein to be phosphorylated sequentially by a defined set of protein kinases.

Recently it was shown that an F-box protein, Fbx13, is re-

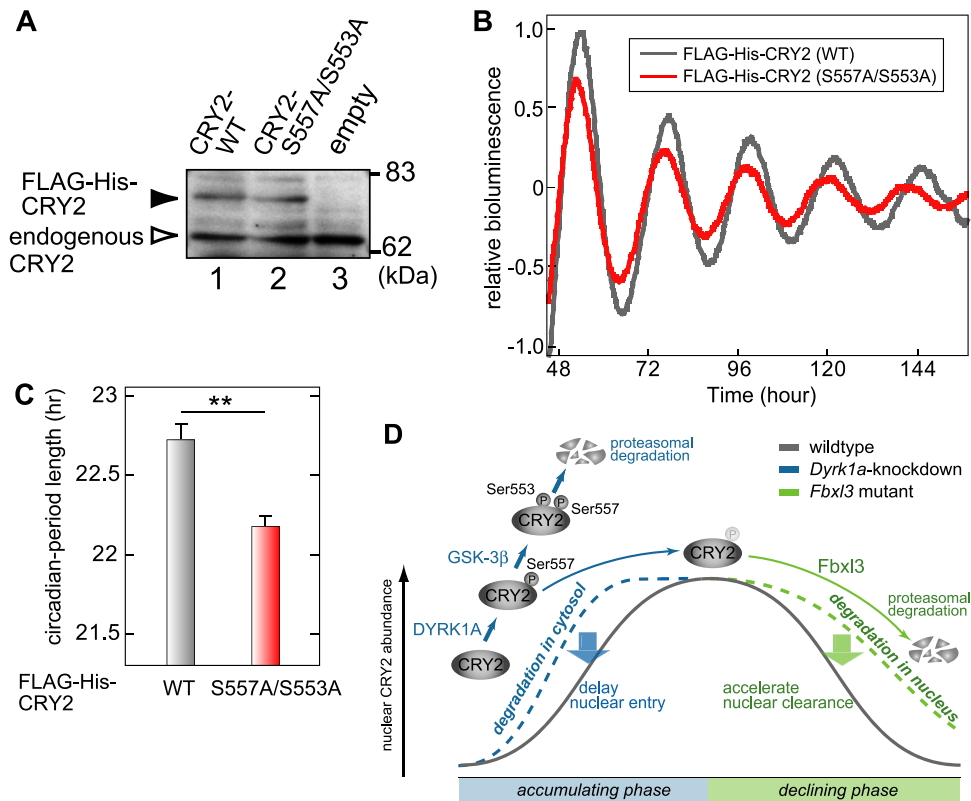


FIG. 6. Alanine mutation of CRY2 at Ser557/Ser553 alters circadian period length. (A) Lysates of NIH 3T3 cells stably expressing FLAG-His-CRY2 were immunoblotted with anti-CRY2 antibody. (B and C) NIH 3T3 cells stably expressing FLAG-His-CRY2 were transiently transfected with the *Bmal1*-luciferase reporter. Twenty-four hours after transfection, the cells were synchronized with dexamethasone treatment for 2 h, and then the luciferase activity was continuously monitored. A representative set of bioluminescence rhythms was shown, and the period lengths of the rhythms were shown with means and SEM ($n = 3$). A double asterisk indicates a P value of 0.01 (by two-tailed Student's t test). (D) A model for spatiotemporally distinct dual degradation mechanism of CRY2.

sponsible for ubiquitination and degradation of both the CRY1 and CRY2 proteins (4, 12, 32). We determined the interaction between expressed Myc-CRY2 and FLAG-Fbxl3 in the presence of MG132. Immunoprecipitation with anti-Myc antibody showed that FLAG-Fbxl3 bound with not only wild-type Myc-CRY2 but also its S557A mutant with apparently similar binding affinities (Fig. 3F). In addition, anti-FLAG antibody coprecipitated nonshifted, upshifted, and super-shifted forms of Myc-CRY2 (Fig. 3G, black, open, and gray arrowheads, respectively). This observation suggests that phosphorylation of CRY2 at Ser557/Ser553 is irrelevant to the interaction between CRY2 and Fbxl3. Consistent with these results, overexpression of Fbxl3 destabilized the S557A mutant to a degree similar to that observed for wild-type CRY2 (Fig. 3H). Thus, Fbxl3 is unlikely to contribute directly to the Ser557/Ser553 phosphorylation-dependent degradation of CRY2. It is most probable that CRY2 is degraded through two distinct mechanisms; one is Ser557/Ser553 phosphorylation-dependent degradation, and the other is Fbxl3-dependent degradation (4, 12, 32).

Because CRY2 functions as a potent inhibitor of E-box-dependent gene expression in the cell nuclei, the fine-tuned timing of accumulation and degradation of nuclear CRY2 should contribute largely to the temporal change of CLOCK-BMAL1 activity, a core part of the clock oscillation (5, 15, 27,

33). A key aspect of the spatiotemporal tuning of the CRY2 protein level involves subcellular distribution of not only CRY2 itself but also the regulatory components for its degradation. Fbxl3 localizes in the nuclei of the cultured cells, supporting that Fbxl3-dependent degradation plays a major role in clearance of nuclear CRY2 (12). In contrast, while DYRK1A activity toward CRY2 is distributed both in the nucleus and the cytosol (Fig. 4D), the GSK-3 β protein was localized mostly in the cytosol of the mouse liver cells (Table 1 and Fig. 4E), highlighting the cytosol as the place where CRY2 Ser553 is phosphorylated. In addition, knockdown of *Dyrk1a* in Rat-1 cells increased both the peak and trough levels of the cytosolic CRY2 protein, accompanying no detectable effect on the protein level of nuclear CRY2 (Fig. 5F). These observations strongly suggest that Ser557/Ser553 phosphorylation event plays a major role in degradation of cytosolic CRY2. Here we should note that the Ser557-phosphorylated form of CRY2, an intermediate form of its degradation process, was undetectable in the cytosol (16). It is most likely that DYRK1A phosphorylation of CRY2 at Ser557 represents a rate-limiting step in the dual phosphorylation-dependent degradation process. Because the activity of DYRK1A toward CRY2 reaches its peak when the CRY2 protein level is increasing (Fig. 4A), the Ser557 phosphorylation-dependent degradation of cytosolic CRY2 should play an active role in the accumulating phase of CRY2.

Based on these observations, we now propose a model in which Ser557/Ser553 phosphorylation-dependent degradation slows down the increasing rate of cytosolic CRY2 in its accumulating phase and enables the timely nuclear entry of CRY2 (Fig. 6D). In fact, *Dyrk1a* knockdown abnormally increased the cytosolic CRY2 protein level over the day, advancing the accumulation timing of nuclear CRY2 (Fig. 5F), and caused shortening of the period length of the cellular clock (Fig. 5D and E). A similar phenotype (a shorter period length) was observed with expression of S557A/S553A-CRY2 (Fig. 6), a mutant that is unable to receive the degradation signal from two clock-regulated protein kinases, DYRK1A and GSK-3 β (Fig. 4A) (16). In line with this, previous studies showed that application of GSK-3 β inhibitors or its knockdown shortens the period length of cellular rhythms (19, 40). Interestingly, *Dyrk1a* knockdown caused the effect of period shortening of ~0.5 h, although it advanced the accumulation timing of nuclear CRY2 as long as 2 to 4 h (Fig. 5). This difference may be explained by the contribution of CRY1, which could have entered into the nuclei at normal timing because it is insensitive to DYRK1A (Fig. 3D). This idea implies that two CRY proteins, in their accumulating phase (i.e., at the onset of suppression of E-box-dependent transcription), may have a cooperative inhibitory function, which may be different from their own activities. On the other hand, in the declining phase of CRY2, we observed no significant extension of the peak time of nuclear CRY2 level in *Dyrk1a*-knocked-down cells despite the high level of the cytosolic CRY2 protein (Fig. 5F). Such a phase-specific effect of *Dyrk1a* knockdown is consistent with marked circadian variations in levels of PER1 and PER2, which serve as nuclear translocators of CRY proteins (24). Collectively, Ser557/Ser553 phosphorylation and the consequent degradation of CRY2 most likely underpin the time-delaying mechanism of the circadian clock oscillation during the accumulating phase of CRY2. In contrast, Godinho et al. (12) suggested that a Fbxl3-dependent degradation mechanism operates specifically in the declining phase of CRY proteins, because a loss-of-function mutation of Fbxl3 causes extension of the CRY-mediated repression phase, which postpones the circadian nadir of PER2 expression, leading to an increase in the period length (12). In the nucleus, Fbxl3-dependent degradation should dominate in the declining phase of CRY2 and determine the diminishing rate of nuclear CRY2. Altogether, the circadian wave of the nuclear CRY2 protein level should be dually governed by spatiotemporally distinct degradation mechanisms (Fig. 6D).

The present study highlights DYRK1A as a novel clock-related protein kinase which governs the cytosolic CRY2 level and the timing of nuclear CRY2 accumulation, enabling the circadian clock to oscillate normally. It also sheds light on sequential phosphorylation mechanisms that are poorly understood in the mammalian clockwork. For *Neurospora*, it is reported that PKA (cAMP-dependent protein kinase) primes for CK-1 α phosphorylation of WC-1 (WHITE COLLAR 1) to strongly inhibit WC complex activity (20). Furthermore, priming phosphorylation of human PER2 at the FASPS site of Ser662, catalyzed by an unidentified kinase, is required for subsequent CKI δ/ϵ phosphorylation and regulation of PER2 stability (42). The sequential phosphorylation of clock proteins would be a key to our understanding of how the posttransla-

tion modifications regulate the pace of the circadian clock oscillation.

During revision of the manuscript, phosphorylation of the CRY1 protein by AMPK (AMP-activated protein kinase) was shown to trigger Fbxl3-dependent degradation (23), a process that is independent of DYRK1A/GSK-3 β -mediated degradation.

ACKNOWLEDGMENTS

We thank Yukiko Gotoh (University of Tokyo) for the *Xenopus* GSK-3 β plasmid, Walter Becker (Medizinische Fakultät der RWTH, Aachen, Germany) for plasmids of GFP-tagged rat DYRK1A, its kinase-negative form, and GST-tagged rat DYRK1A, and Hikari Yoshitane for comments on the manuscript.

This work was supported in part by Grants-in-Aid for Scientific Research and by the 21st century COE and Global COE program (Integrative Life Science Based on the Study of Biosignaling Mechanisms) from MEXT, Japan. N.K. is supported by JSPS Research Fellowships for Young Scientists.

REFERENCES

1. Akashi, M., Y. Tsuchiya, T. Yoshino, and E. Nishida. 2002. Control of intracellular dynamics of mammalian period proteins by casein kinase I ϵ (CKI ϵ) and CKI δ in cultured cells. *Mol. Cell. Biol.* **22**:1693–1703.
2. Arron, J. R., M. M. Winslow, A. Polleri, C. Chang, H. Wu, X. Gao, J. R. Neilson, L. Chen, J. J. Heit, S. K. Kim, N. Yamsaki, T. Miyakawa, U. Francke, I. A. Graef, and G. R. Crabtree. 2006. NFAT dysregulation by increased dosage of DSCR1 and DYRK1A on chromosome 21. *Nature* **441**:595–600.
3. Bungler, M. K., L. D. Wilsbacher, S. M. Moran, C. Clendenin, L. A. Radcliffe, J. B. Hogenesch, M. C. Simon, J. S. Takahashi, and C. A. Bradfield. 2000. Mop3 is an essential component of the master circadian pacemaker in mammals. *Cell* **103**:1009–1017.
4. Busino, L., F. Bassermann, A. Maiolica, C. Lee, P. M. Nolan, S. I. Godinho, G. F. Draetta, and M. Pagano. 2007. SCF^{Fbxl3} controls the oscillation of the circadian clock by directing the degradation of cryptochrome proteins. *Science* **316**:900–904.
5. Dunlap, J. C. 1999. Molecular bases for circadian clocks. *Cell* **96**:271–290.
6. Eide, E. J., M. F. Woolf, H. Kang, P. Woolf, W. Hurst, F. Camacho, E. L. Vielhaber, A. Giovanni, and D. M. Virshup. 2005. Control of mammalian circadian rhythm by CKI ϵ -regulated proteasome-mediated PER2 degradation. *Mol. Cell. Biol.* **25**:2795–2807.
7. Fotaki, V., M. Dierssen, S. Alcantara, S. Martine, E. Marti, C. Casas, J. Visa, E. Soriano, X. Estivill, and M. L. Arbones. 2002. *Dyrk1A* haploinsufficiency affects viability and causes developmental delay and abnormal brain morphology in mice. *Mol. Cell. Biol.* **22**:6636–6647.
8. Frame, S., and P. Cohen. 2001. GSK3 takes centre stage more than 20 years after its discovery. *Biochem. J.* **359**:1–16.
9. Gallego, M., E. J. Eide, M. F. Woolf, D. M. Virshup, and D. B. Forger. 2006. An opposite role of *tau* in circadian rhythm revealed by mathematical modeling. *Proc. Natl. Acad. Sci. U. S. A.* **103**:10618–10623.
10. Gallego, M., and D. M. Virshup. 2007. Post-translational modifications regulate the ticking of the circadian clock. *Nat. Rev. Mol. Cell Biol.* **8**:139–148.
11. Gekakis, N., D. Staknis, H. B. Nguyen, F. C. Davis, L. D. Wilsbacher, D. P. King, J. S. Takahashi, and C. J. Weitz. 1998. Role of the CLOCK protein in the mammalian circadian mechanism. *Science* **280**:1564–1569.
12. Godinho, S. I., E. S. Maywood, L. Shaw, V. Tucci, A. R. Barnard, L. Busino, M. Pagano, R. Kendall, M. M. Quailid, M. R. Romero, J. O'Neill, J. E. Chesham, D. Brooker, Z. Lalanne, M. H. Hastings, and P. M. Nolan. 2007. The after-hours mutant reveals a role for Fbxl3 in determining mammalian circadian period. *Science* **316**:897–900.
13. Guimera, J., C. Casas, X. Estivill, and M. Pritchard. 1999. Human minibrain homologue (MNBH/DYRK1): characterization, alternative splicing, differential tissue expression, and overexpression in Down syndrome. *Genomics* **57**:407–418.
14. Gwack, Y., S. Sharma, J. Nardone, B. Tanasa, A. Iuga, S. Srikanth, H. Okamura, D. Bolton, S. Feske, P. G. Hogen, and A. Rao. 2006. A genome-wide *Drosophila* RNAi screen identifies DYRK-family kinase as regulators of NFAT. *Nature* **441**:646–650.
15. Hall, J. C. 2000. Cryptochromes: sensory reception, transduction, and clock functions subserving circadian systems. *Curr. Opin. Neurobiol.* **10**:456–466.
16. Harada, Y., M. Sakai, N. Kurabayashi, T. Hirota, and Y. Fukada. 2005. Ser-557-phosphorylated mCRY2 is degraded upon synergistic phosphorylation by glycogen synthase kinase-3 β . *J. Biol. Chem.* **280**:31714–31721.
17. Himpel, S., P. Panzer, K. Eirnbter, H. Czajkowska, M. Sayed, L. C. Packman, T. Blundell, H. Kentrup, J. Grötzinger, H. G. Joost, and W. Becker.

2001. Identification of the autophosphorylation sites and characterization of their effects in the protein kinase DYRK1A. *Biochem. J.* **359**:497–505.
18. Himpel, S., W. Tegge, R. Frank, S. Leder, H. G. Joost, and W. Becker. 2000. Specificity determinants of substrate recognition by the protein kinase DYRK1A. *J. Biol. Chem.* **275**:2431–2438.
 19. Hirota, T., W. G. Lewis, A. C. Liu, J. W. Lee, P. G. Schultz, and S. A. Kay. 2008. A chemical biology approach reveals period shortening of the mammalian circadian clock by specific inhibition of GSK-3 β . *Proc. Natl. Acad. Sci. U. S. A.* **105**:20746–20751.
 20. Huang, G., S. Chen, S. Li, J. Cha, C. Long, L. Li, Q. He, and Y. Liu. 2007. Protein kinase A and casein kinases mediate sequential phosphorylation events in the circadian negative feedback loop. *Genes Dev.* **21**:3283–3295.
 21. Kon, N., T. Hirota, T. Kawamoto, Y. Kato, T. Tsubota, and Y. Fukada. 2008. Activation of TGF-beta/activin signaling resets the circadian clock through rapid induction of *Dec1* transcripts. *Nat. Cell Biol.* **10**:1463–1469.
 22. Kume, K., M. J. Zylka, S. Sriram, L. P. Shearman, D. R. Weaver, X. Jin, E. S. Maywood, M. H. Hastings, and S. M. Reppert. 1999. mCRY1 and mCRY2 are essential components of the negative limb of the circadian clock feedback loop. *Cell* **98**:193–205.
 23. Lamia, K. A., U. M. Sachdeva, L. DiTacchio, E. C. Williams, J. G. Alvarez, D. F. Egan, D. S. Vasquez, H. Juguilon, S. Panda, R. J. Shaw, C. B. Thompson, and R. M. Evans. 2009. AMPK regulates the circadian clock by cryptochrome phosphorylation and degradation. *Science* **326**:437–440.
 24. Lee, C., J. P. Etchegaray, F. R. Cagampang, A. S. Loudon, and S. M. Reppert. 2001. Posttranslational mechanisms regulate the mammalian circadian clock. *Cell* **107**:855–867.
 25. Okui, M., T. Ide, K. Morita, E. Funakoshi, F. Ito, K. Ogita, Y. Yoneda, J. Kudoh, and N. Shimizu. 1999. High-level expression of the *Mnb/Dyrk1A* gene in brain and heart during rat early development. *Genomics* **62**:165–171.
 26. Pagano, M. A., G. Poletto, G. D. Maira, G. Cozza, M. Ruzzene, S. Sarno, J. Bain, M. Elliott, S. Moro, G. Zagotto, F. Meggio, and L. A. Pinna. 2007. Tetrabromocinnamic acid (TBCA) and related compounds represent a new class of specific protein kinase CK2 inhibitors. *ChemBioChem* **8**:129–139.
 27. Reppert, S. M., and D. R. Weaver. 2002. Coordination of circadian timing in mammals. *Nature* **418**:935–941.
 28. Sanada, K., Y. Harada, M. Sakai, T. Todo, and Y. Fukada. 2004. Serine phosphorylation of mCRY1 and mCRY2 by mitogen-activated protein kinase. *Genes Cells* **9**:697–708.
 29. Sarno, S., H. Reddy, F. Meggio, M. Ruzzene, S. P. Davies, A. Donella-Deana, D. Shugar, and L. A. Pinna. 2001. Selectivity of 4,5,6,7-tetrabromobenzotriazole, an ATP site-directed inhibitor of protein kinase CK2 ('casein kinase-2'). *FEBS Lett.* **496**:44–48.
 30. Shearman, L. P., S. Sriram, D. R. Weaver, E. S. Maywood, I. Chaves, B. Zheng, K. Kume, C. C. Lee, van der G. T. Horst, M. H. Hastings, and S. M. Reppert. 2000. Interacting molecular loops in the mammalian circadian clock. *Science* **288**:1013–1019.
 31. Shirogane, T., J. Jin, X. L. Ang, and J. W. Harper. 2005. SCF^{beta-TRCP} controls clock-dependent transcription via casein kinase 1-dependent degradation of the mammalian period-1 (Per1) protein. *J. Biol. Chem.* **280**:26863–26872.
 32. Siepkka, S. M., S. H. Yoo, J. Park, W. Song, V. Kumar, Y. Hu, C. Lee, and J. S. Takahashi. 2007. Circadian mutant Overtime reveals F-box protein FBXL3 regulation of cryptochrome and period gene expression. *Cell* **129**:1011–1023.
 33. Takahashi, J. S. 1995. Molecular neurobiology and genetics of circadian rhythms in mammals. *Annu. Rev. Neurosci.* **18**:531–553.
 34. Takano, A., Y. Isojima, and K. Nagai. 2004. Identification of mPer1 phosphorylation sites responsible for the nuclear entry. *J. Biol. Chem.* **279**:32578–32585.
 35. Takano, A., M. Uchiyama, N. Kajimura, K. Mishima, Y. Inoue, Y. Kamei, T. Kitajima, K. Shibui, M. Katoh, T. Watanabe, Y. Hashimoto-dani, T. Nakajima, Y. Ozeki, T. Hori, N. Yamada, R. Toyoshima, N. Ozaki, M. Okawa, K. Nagai, K. Takahashi, Y. Isojima, T. Yamauchi, and T. Ebisawa. 2004. A missense variation in human casein kinase I epsilon gene that induces functional alteration and shows an inverse association with circadian rhythm sleep disorders. *Neuropsychopharmacology* **29**:1901–1909.
 36. Toh, K. L., C. R. Jones, Y. He, E. J. Eide, W. A. Hinz, D. M. Virshup, L. J. Ptáček, and Y. H. Fu. 2001. An hPer2 phosphorylation site mutation in familial advanced sleep phase syndrome. *Science* **291**:1040–1043.
 37. van der Horst, G. T., M. Muijtjens, K. Kobayashi, R. Takano, S. Kanno, M. Takao, de J. Wit, A. Verkerk, A. P. Eker, D. van Leenen, R. Buijs, D. Bootsma, J. H. Hoeijmakers, and A. Yasui. 1999. Mammalian *Cry1* and *Cry2* are essential for maintenance of circadian rhythms. *Nature* **398**:627–630.
 38. Vanselow, K., J. T. Vanselow, P. O. Westermarck, S. Reischl, B. Maier, T. Korte, A. Herrmann, H. Herzl, A. Schlosser, and A. Kramer. 2006. Differential effects of PER2 phosphorylation: molecular basis for the human familial advanced sleep phase syndrome (FASPS). *Genes Dev.* **20**:2660–2672.
 39. Vitaterna, M. H., C. P. Selby, T. Todo, H. Niwa, C. Thompson, E. M. Fruechte, K. Hitomi, R. J. Thresher, T. Ishikawa, J. Miyazaki, J. S. Takahashi, and A. Sancar. 1999. Differential regulation of mammalian period genes and circadian rhythmicity by cryptochromes 1 and 2. *Proc. Natl. Acad. Sci. U. S. A.* **96**:12114–12119.
 40. Vougiannopoulou, K., Y. Ferandin, K. Bettayeb, V. Myrianthopoulos, O. Lozach, Y. Fan, C. H. Johnson, P. Magiatis, A.-L. Skaltsounis, E. Mikros, and L. Meijer. 2008. Soluble 3',6-substituted Indirubins with enhanced selectivity toward glycogen synthase kinase-3 alter circadian period. *J. Med. Chem.* **51**:6421–6431.
 41. Xu, Y., Q. S. Padiath, R. E. Shapiro, C. R. Jones, S. C. Wu, N. Saigoh, K. Saigoh, L. J. Ptáček, and Y. H. Fu. 2005. Functional consensus of a CKI δ mutation causing familial advanced sleep phase syndrome. *Nature* **434**:640–644.
 42. Xu, Y., K. L. Toh, C. R. Jones, J. Y. Shin, Y. H. Fu, and L. J. Ptáček. 2007. Modeling of a human circadian mutation yields insights into clock regulation by PER2. *Cell* **128**:59–70.
 43. Yamazaki, S., R. Numano, M. Abe, A. Hida, R. Takahashi, M. Ueda, G. D. Block, Y. Sakaki, M. Menaker, and H. Tei. 2000. Resetting central and peripheral circadian oscillators in transgenic rats. *Science* **288**:682–685.
 44. Yoshitane, H., T. Takao, Y. Satomi, N. H. Du, T. Okano, and Y. Fukada. 2009. Roles of CLOCK phosphorylation in suppression of E-box-dependent transcription. *Mol. Cell. Biol.* **29**:3675–3686.